

Multi-stage Multi-energy Flow Integrated Energy Systems of Electricity, Gas, and Heat Based on Heterogeneous Energy Flow Characteristics

Qinglong Gou^{1,a}, Yansong Wang^{1,b*}, Qingzeng Yan^{1,c}

¹College of New Energy, China University of Petroleum (East China), Qingdao 266580, China

Abstract

INTRODUCTION: The development of integrated energy systems (IES) is of paramount significance in addressing climate change and other challenges. Ensuring the rapid and accurate calculation of energy flow states is crucial for their efficient operation. However, the difference in response time of various heterogeneous energy flows in IES will lead to the inaccuracy of the steady-state model.

OBJECTIVES: This paper proposes a model for multi-stage multi-energy flow IES of electricity, gas, and heat based on heterogeneous energy flow characteristics.

Methods: IES was divided into fast variable networks and slow variable networks, and a multi-energy flow multi-stage model was established. Suitable models were matched for different subnets at different stages to improve the calculation accuracy.

RESULTS: Selected a practical Electrical-Gas-Heat IES as a case study for simulation. Through case studies, the effectiveness and accuracy of the proposed method are demonstrated.

CONCLUSION: The multi-stage model proposed in this paper can improve the accuracy of multi-energy flow in IES.

Keywords: Integrated Energy Systems, Multi-Energy Flow, Multi-Stage, Power Flow Calculation

Received on 15 November 2023, accepted on 09 April 2024, published on 16 April 2024

Copyright © 2024 Q. Guo *et al.*, licensed to EAI. This is an open access article distributed under the terms of the [CC BY-NC-SA 4.0](https://creativecommons.org/licenses/by-nc-sa/4.0/), which permits copying, redistributing, remixing, transformation, and building upon the material in any medium so long as the original work is properly cited.

doi: 10.4108/ew.5799

1. Introduction

In recent years, there has been an increasing global concern regarding issues such as climate change, environmental pollution, and energy crisis [1-4]. To address these challenges, engineers, researchers, and scientists have been continuously exploring solutions [5]. Research has revealed that a substantial portion of electricity is dedicated to heating applications in energy utilization. For instance, in India, more than 70% of the electricity demand is attributed to heating purposes [6]. Nevertheless, the adoption of combined heat and power (CHP) technology enables the achievement of over 90% high fuel efficiency [7], while effectively reducing the emissions of environmental pollutants [8] and greenhouse gases [9]. Furthermore, the utilization of gas turbines and the development of power-to-gas (P2G) technology provide assurance for stabilizing

intermittent renewable energy generation [10]. IES based on the complementary characteristics of various energy sources such as electricity, heat, and gas, as well as the principle of cascaded energy utilization, offer a crucial approach for the unified planning and coordinated optimization of multi-energy systems, thereby enhancing energy efficiency [11]. In the current context, the development of IES has become a key pathway to meet the energy demands [12].

However, IES involve multiple energy flows, each with different transmission speeds [13]. This temporal disparity poses a challenge for traditional steady-state models to meet the real-time scheduling requirements of electricity-gas-heat coupled IES. Therefore, it is of great significance to study dynamic power flow algorithms based on heterogeneous energy flow characteristics [14].

Currently, research on the IES model is continuously advancing. References [15-17] address the dynamic characteristics of heat networks, such as delay and heat storage, and propose a pipe network heat storage model by combining it with a dynamic model of the heat network.

^a1806030406@s.upc.edu.cn, ^{b*}Corresponding author: wys91517@163.com, ^cyanqingzeng@upc.edu.cn3

Additionally, references [18-20] investigate dynamic computation methods for gas networks. Although the aforementioned studies have made progress in terms of model accuracy, they only focus on the coupling between individual sub-networks and the electricity power network, lacking a comprehensive consideration of the electricity-gas-heat IES as a whole. Reference [21] divides the interaction process of IES into four quasi-steady-state stages and discusses the bidirectional coupling of IES. However, for the heat network, only steady-state models are used for analysis. Although the time-varying nature of the heat network is considered, the state of IES when the heat network has not reached a steady state cannot be analyzed. Reference [22] investigates the coupling relationships and interactions among different sub-networks in the electricity-gas-heat IES, as well as the differences in dynamic characteristics between different networks. However, the study overlooks the influence of heat network storage and time delay characteristics and does not consider the impact of stored hot water in the heat network on the power of the CHP unit during heat network quality regulation.

Given this, the aim of this paper is to analyze the energy flow characteristics and interaction mechanisms of various sub-networks in IES and propose a multi-stage model for multi-energy flow calculation. Firstly, considering the energy flow characteristics of each sub-network and the actual minimum scheduling interval, the sub-networks are divided into fast-varying networks and slow-varying networks. Then, considering the interaction mechanisms and the state of the slow-varying system in IES, IES is divided into three stages. Finally, the applicable models for each stage of the sub-networks and the conditions for stage transitions are analyzed. The effectiveness of the proposed model is verified through comparative analysis of the accuracy of the calculated results. The main contributions of this paper are as follows:

- (i) To achieve accurate computation results in IES, IES is divided into three stages, and the sub-networks are divided into slow-varying networks and fast-varying networks. The current stage of IES is determined based on the state of the slow-varying network and the output of coupling elements.
- (ii) The proposed model are validated in the electricity-gas-heat IES system.

2. Multi-stage model of Electricity-Gas-Heat IES

2.1 Architecture of electricity-gas-heat IES

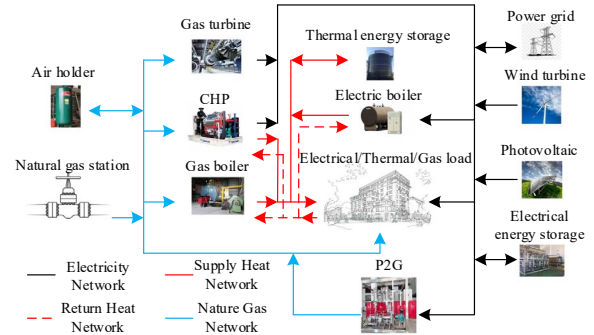


Figure 1. Structure of IES

IES generally comprise five main components: sources, networks, loads, storage, and coupling elements, as depicted in Figure 1. It is worth noting that the electrical grid source and gas grid source are considered infinite sources, whereas the heat grid source is treated as a coupling element and does not possess infinite characteristics. Extensive research has been conducted worldwide on the modeling of these networks and elements [15-20,23], which will not be further elaborated in this paper.

2.2 IES multi-stage multi-energy flow model

Analysis of IES interaction mechanism

The interaction mechanism of IES can be classified into one-way coupling and two-way coupling [21]. In one-way coupling, the perturbation from Network A is transmitted to Network B through the coupling element without any feedback affecting Network A, as shown in Figure 2(a). In two-way coupling, the perturbation from Network A is transmitted to Network B through the coupling element, and the response from Network B can directly or indirectly feedback and influence Network A, as shown in Figure 2(b) and Figure 2(c).

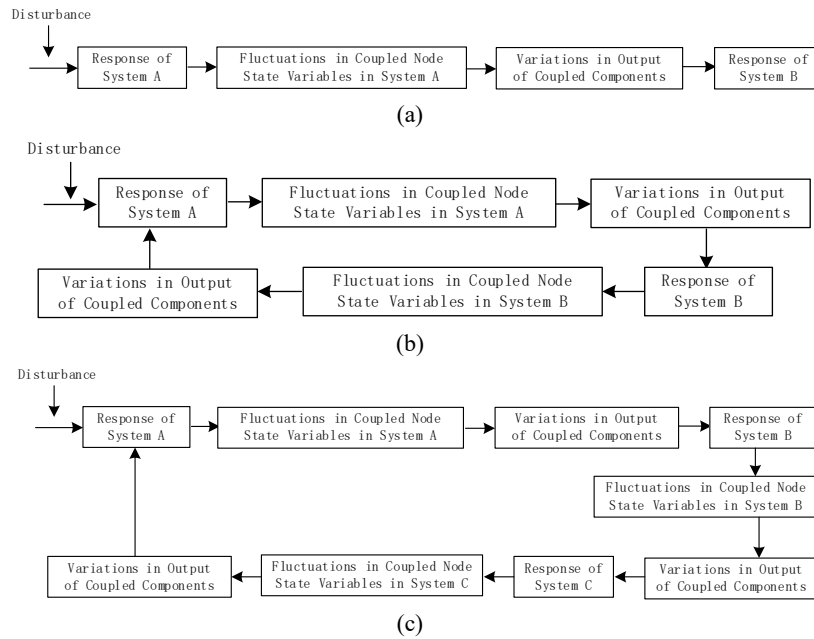


Figure 2. IES interaction mechanism diagram

Regardless of whether it is one-way coupling or two-way coupling, the response of the networks is achieved through changes in the output of the coupling elements. If $P_{CC}^t \neq P_{CC}^{t+1}$, P_{CC} is the output of the coupling elements, the system is classified as being in the dynamic stage. Conversely, $P_{CC}^t = P_{CC}^{t+1}$, it is categorized as being in the steady-state/quasi-steady-state stage.

IES Multi-time scale characteristics

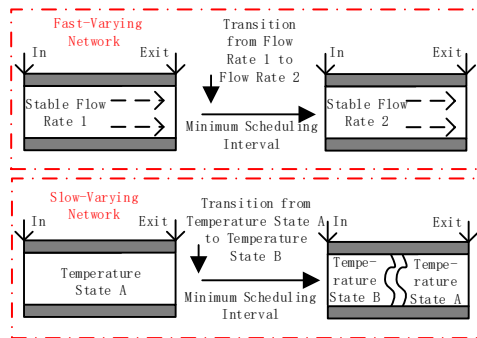


Figure 3. The schematic diagram of fast-varying networks and slow-varying networks

In the electricity-gas-heat coupled network, there are significant differences in the dynamic response time of each

sub-network. The dynamic response time of the electricity and water networks is typically in the range of seconds to minutes, while the dynamic response time of the gas and heat networks is usually in the range of minutes to hours [22]. To meet the requirements of practical scheduling, we divide the sub-networks into fast-varying networks and slow-varying networks based on the actual minimum scheduling interval, which exhibit differences between the two networks, as shown in Figure 3. For sub-networks that can reach a new steady state within the minimum scheduling interval, we use the steady-state model for computation. For sub-networks that cannot reach a new steady state within the minimum scheduling interval, we employ a computation method that combines the steady-state model and the dynamic model.

State judgment of slow-varying network

The minimum interval between system schedules usually ranges from a few minutes to a few hours. Therefore, the slow-varying network discussed in this paper only includes gas network and heat network.

Figure 4 illustrates the changes occurring in the slow-varying network pipelines following scheduling.

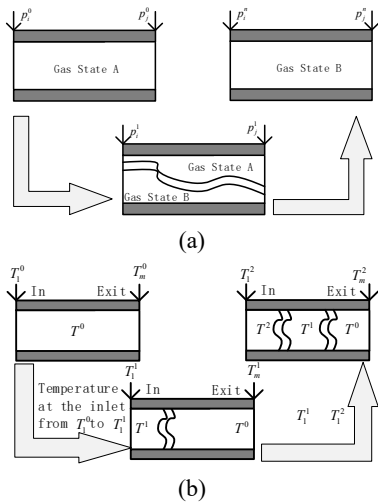


Figure 4. Schematic diagram of IES slow-varying network pipeline change

Figure 4(a) illustrates the schematic diagram depicting the changes in the state of the gas network pipelines before and after scheduling. In the diagram, p_i^0 and p_j^0 represent the gas pressure at the two ends of the pipeline before scheduling, while p_i^1 and p_j^1 represent the gas pressure at the two ends of the pipeline during the scheduling process. Additionally, p_i^n and p_j^n represent the gas pressure at the two ends of the pipeline after achieving stability. If $\forall i, \exists p_i^1 = p_i^n$, it can be determined that the gas network has reached a steady state.

Figure 4(b) illustrates the changes occurring in the heat network pipelines following scheduling. The subscript in the bottom right corner denotes the position number of the hot water within the pipeline, while the subscript in the top right corner represents the current scheduling iteration. When $T_i^0 \neq T_i^1$ and $T_m^0 = T_m^2$, if the pipeline is sufficiently long to ensure $T_m^0 = T_m^1 = T_m^2$, even though the temperatures at each node conform to the steady-state model, the heat network is not in a steady state. Hence, it is only by aligning the temperature of each microelement within the pipeline with the steady-state model, denoted as $\forall x \in [1, m], T_x = T_x^n$, where T_x^n represents the temperature of the hot water at position x in the steady state, that a determination can be made regarding whether the heat network is in a steady state.

IES State Phases

In an IES, there are notable variations in the energy flow characteristics among different subsystems, and their response speeds differ as well. Each subsystem requires a different amount of time to reach a steady state after disturbances or faults. Relying solely on steady-state analysis while disregarding the dynamic processes can have

adverse effects on the accuracy and economic efficiency of scheduling. However, conducting precise dynamic analysis of an IES requires a considerable amount of time for system simulation, making it challenging to meet the demand for fast system calculations. To address the need for both accuracy and speed in IES simulation, this study proposes dividing the IES into distinct states and determining whether to employ steady-state models for calculation based on the variations in output from coupled components and the feasibility of approximating slow-varying networks using steady-state models. As depicted in Figure 5, this study categorizes the IES into the dynamic stage, quasi-steady stage, and steady-state stage.

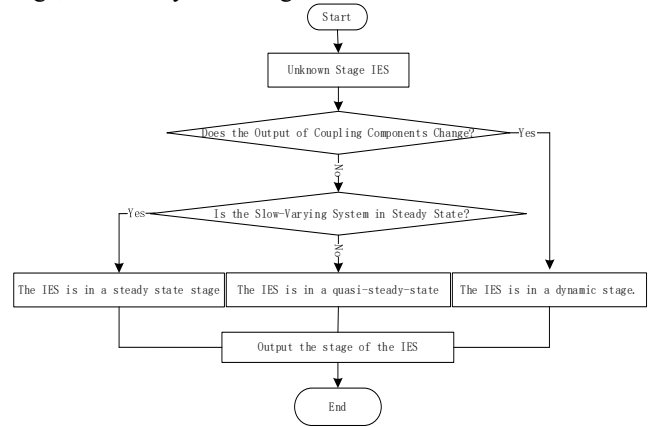


Figure 5. Schematic diagram of phase division

3. Case Study

3.1 Introduction of calculation examples

We selected a practical Electrical-Gas-Heat IES as a case study for simulation. As depicted in Figure 6, this system couples three subsystems: the electrical network, the heat network, and the natural gas network, through the utilization of two CHP. In the figure 6, GB, HB and EB represent natural gas, heat and electricity network nodes.

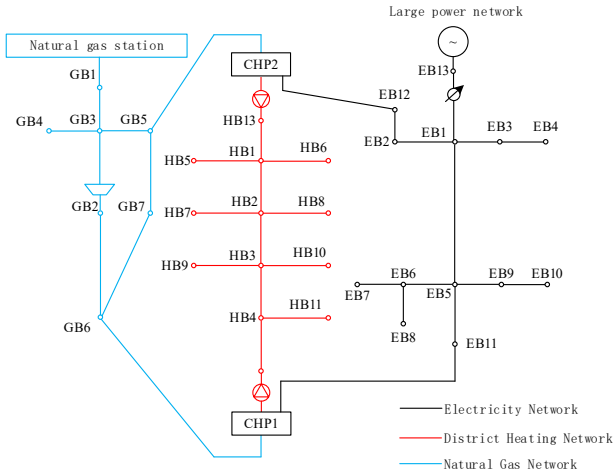


Figure 6. IES node topology

The natural gas network incorporates a compressor with a known outlet pressure. For detailed parameters of the IES, please refer to the reference [23].

During the simulation, we linked node EB13 to the main power grid as the reference node, while nodes EB11 and EB12 were assigned as PV nodes. The CHP operated in a heat-led mode, with node HB13 serving as the reference node for the heat network, and GB1 as the reference node for the natural gas network.

We conducted scheduling simulation calculations using both the steady-state model method and the multi-stage model method, with simulation spanning a total duration of 48 hours. The results were compared between the two methods. The scheduling interval was set to 1 hour, and the variation of the heat load in the network is illustrated in Figure 7. The heat network is regulated by adjusting the water supply temperature of the heat source.

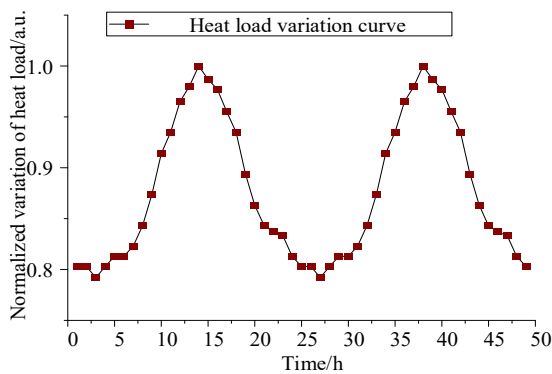


Figure 7. Variation of Network Heat Load

3.2 Model Comparison

In the graph, we normalized the data for each node, using the value of the steady-state model at that node when the heat load is 1 as the reference value.

Coupling element output change

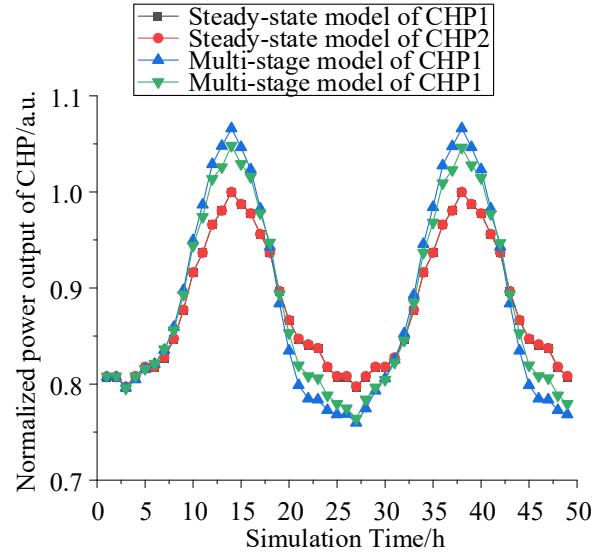


Figure 8. CHP output per unit value change

Based on the results shown in Figure 8, it can be observed that the normalized variation of CHP power in the steady-state model aligns with the heat load curve. However, in the multi-stage model, the normalized variation of CHP power exceeds that of the heat load curve. In other words, when subjected to the same load fluctuation, the change in CHP unit power calculated using the multi-stage model is greater than the results obtained from the steady-state model. This disparity arises because the steady-state model fails to consider the influence of the current moment's return water temperature due to the heat network pipeline inventory. Due to the lower initial pipe water temperature on the first day compared to the second day, the power output of the CHP exceeded that of hours 25 to 29 during the period of 0 to 4 hours. This difference in CHP power is regarded as the energy storage characteristic of the heat network during scheduling. When the heat source temperature increases, the temperature of the stored hot water in the heat network pipeline rises, indicating heat storage, and the heat output of the heat source surpasses the heat consumption of the heat load. Conversely, when the heat source temperature decreases, the temperature of the stored hot water in the heat network pipeline decreases, indicating heat release, and the heat output of the heat source falls below the heat consumption of the heat load.

Node State Changes

Due to space constraints, we conducted an analysis on a selection of representative nodes.

This phenomenon is attributed to the lag in heat transfer and the diffusion of heat in the heat network. Figure 9 illustrates that when there is a variation in the temperature of the hot water supply from the heat source, the temperatures of nodes HB1, HB2, and HB3 remain constant for a certain period before eventually undergoing changes. This behavior exemplifies the lag in heat transfer within the heat network. HB1 is the node closest to the heat source node HB13. Due to its proximity to the heat source node HB13 and the shorter length of pipeline 1 connecting these two nodes, HB1 can evacuate all the retained hot water in the pipeline from the previous scheduling within a 1-hour scheduling interval. Hence, the temperature curves obtained from both the quasi-steady-state model and the steady-state model for HB1 are identical. This implies that when the delay time of the pipeline is smaller than the scheduling interval, the diffusion of heat can be neglected.

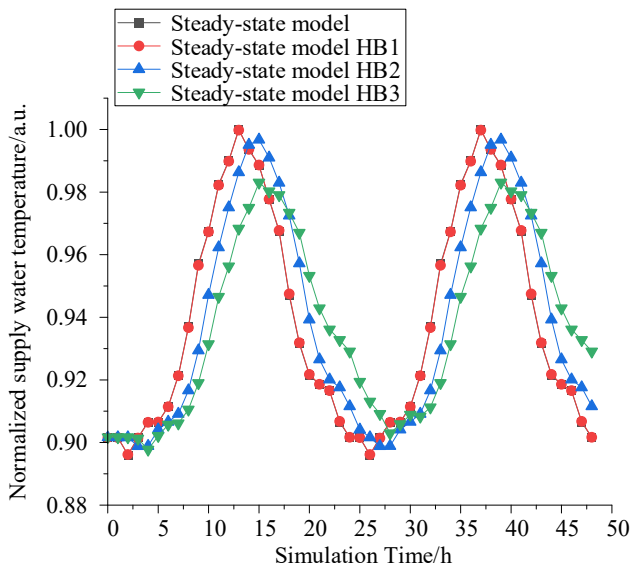


Figure 9. Normalized Variation of Supply Water Temperature in the Heat Network

In contrast, HB2 is located further away from the heat source node HB13 compared to HB1. The hot water from HB13 needs to pass through pipeline 1 and pipeline 2 before reaching HB2. Within a 1-hour scheduling interval, it is not feasible to completely evacuate all the previously retained hot water in the pipeline from the previous scheduling. Consequently, the theoretical peak value of the steady-state calculation cannot be achieved, which is a result of the heat diffusion effect. Hence, there exist differences in the temperature curves obtained from the quasi-steady-state model and the steady-state model for HB2.

The significant decrease in the peak value of HB3 can be attributed to the aforementioned reasons, as well as the fact that it serves as a flow convergence node. The temperature

at this node is determined by the outlet water temperatures of two pipelines. Moreover, the hot water takes different amounts of time to reach the node through these two distinct pipelines. Consequently, when the water temperature at the 4-3 pipeline reaches its peak, the temperature at the 2-3 pipeline has not yet reached its peak. Similarly, when the temperature at 2-3 reaches its peak, the temperature at 4-3 has not yet reached its peak. Therefore, there exist differences in the temperature curves obtained from steady-state model, the quasi-steady-state model for HB1, and the quasi-steady-state model for HB2, as well as the quasi-steady-state model for HB3.

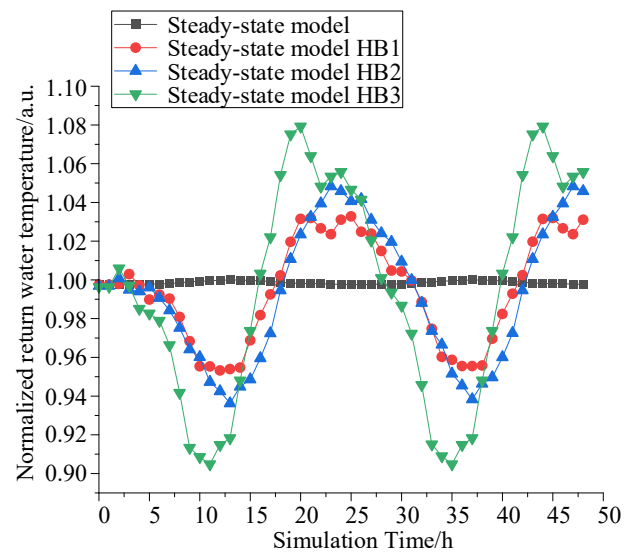


Figure 10. Normalized Variation of Return Water Temperature in the Heat Network

Based on the results shown in Figure 10, it can be observed that in the steady-state model, the return water temperature remains relatively constant. However, in the multi-stage model, the return water temperature exhibits larger fluctuations compared to the steady-state model. This phenomenon can be attributed to the lag in heat transfer. When there is a change in the heat load, the supply water temperature at the heat load nodes does not adjust accordingly, resulting in a certain deviation between the actual return water temperature and the calculated results of the steady-state model.

As a result of the deviation in the return water temperature at the heat load nodes, when the hot water flows towards downstream return water nodes, it further deviates from the predicted values of the steady-state model. This is also the underlying reason why the return water temperature curves at nodes HB1, HB2, and HB3 differ between the multi-stage model and the steady-state model, and why their temperature curves are also distinct from one another.

Comparison of Extreme Values in Heat Network Nodes

By observing Figure 11, it can be observed that in the multi-stage model calculations, the difference in peak values between the supply water temperature of the nodes and the results obtained from the steady-state model is relatively small. However, the difference in peak values between the return water temperature of the nodes and the results obtained from the steady-state model is relatively large. The main reason for this phenomenon is that in the supply water network, the lag in heat transfer does not affect the maximum and minimum temperatures, except for the convergence node HB3 and the nodes HB9 and HB10 following the convergence node. For other nodes in the heat network, the maximum and minimum temperatures are primarily influenced by the diffusion of heat. However, in the return water network, the lag in heat transfer leads to a mismatch between the actual supply water temperature at the heat load nodes and the current load. This mismatch results in an error between the actual return water temperature and the calculated results from the steady-state model, leading to larger fluctuations in the return water temperature of the nodes in the multi-stage model.

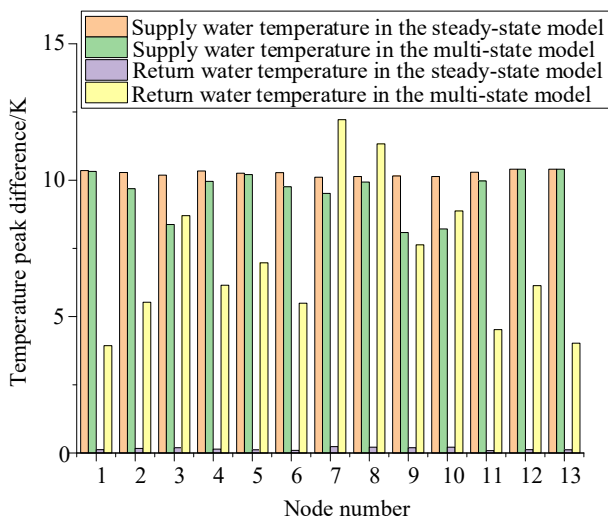


Figure 11. Peak Difference of Water Temperature in Heat Network Nodes

4. Conclusion

This paper analyzes the energy flow characteristics and interaction mechanisms of the electricity-gas-heat IES subnetwork. Taking into account the energy flow characteristics of each subnetwork and the actual minimum scheduling interval, the subnetworks are divided into fast-varying networks and slow-varying networks. Additionally, considering the interaction mechanisms and the slow-varying system state of the IES, the IES is divided into three stages. The applicable models for each stage of the subnetworks and the conditions for stage transitions are

analyzed. Based on this method, a multi-energy flow multi-stage power flow model for electricity-gas-heat systems is constructed. Based on the results of numerical examples, the following conclusions are drawn:

- (i) In the quasi-steady-state stage, the lag in heat transfer results in larger changes in the output of the heat source during load regulation compared to the actual variation in heat load. During the heating control, the excess heat is utilized to raise the temperature of the stored hot water. Conversely, during the cooling control, due to the insufficient heat, heat needs to be extracted from the stored hot water to compensate for the deficit.
- (ii) During the quasi-steady state phase, the delayed heat transfer and the diffusive effect of heat energy in the heating network result in the actual peak value of the supply water temperature being lower than the value predicted by the steady-state model. Conversely, due to the lag in heat transfer, the return network causes a mismatch between the real-time supply water temperature at the nodes and the heat load, leading to the actual peak value of the return water temperature being higher than the value predicted by the steady-state model.

Acknowledgements

This work was supported in part by the National Natural Science Foundation of China under Project (52277208), the Key R&D Program of Shandong Province, China (2019GGX103045), and supported by the Fundamental Research Funds for the Central Universities under Project (23CX07012A).

References

- [1] Zhu Hongyu, Goh Hwang Hui, Zhang Dongdong, Ahmad Tanveer, Liu Hui, Wang Shuyao, Li Shenwang, Liu Tianhao, Dai Hang, Wu Thomas. Key technologies for smart energy systems: Recent developments, challenges, and research opportunities in the context of carbon neutrality[J]. *Journal of Cleaner Production*. 2022;331:20.
- [2] Busu, Mihai. The Role of Renewables in a Low-Carbon Society: Evidence from a Multivariate Panel Data Analysis at the EU Level[J]. *Sustainability*. 2019;11:16.
- [3] Zhao Wenhui, Zou Ruican, Yuan Guanghui, Wang Hui, Tan, Zhongfu. Long-Term Cointegration Relationship between China's Wind Power Development and Carbon Emissions[J]. *Sustainability*. 2019; 11:12.
- [4] Gizaw, Mintesnot, Bekele, Getachew. Investigation of Sustainable Technology Options: Wind, Pumped-hydro-storage and Solar potential to Electrify Isolated Ziway Islanders in Ethiopia[J]. *EAI Endorsed Transactions on Energy Web*. 2023;10:12.
- [5] Erixno Oon, Abd Rahim Nasrudin, Ramadhani Farah, Adzman Noriah Nor. Energy management of renewable energy-based combined heat and power systems: A review[J]. *Sustainable Energy Technologies and Assessments*. 2022; 51:25.
- [6] Subramani R., Vijayalakshmi C.. Augmented Lagrangian algorithm for hydrothermal scheduling[J]. *EAI Endorsed Transactions on Energy Web*. 2018;5:7.
- [7] Gustafsson Jonas, Delsing Jerker, van Deventer Jan. Improved district heating substation efficiency with a new control strategy[J]. *Applied Energy*. 2010;87(6):1996-2004.

- [8] Karki, Shankar, Kulkarni Manohar, Mann, Michael D., Salehfar, Hossein. Efficiency improvements through combined heat and power for onsite distributed generation technologies[J]. *Cogeneration & Distributed Generation Journal*.2007;22(3):19-34.
- [9] Hast Aira, Syri Sanna, Lekavicius Vidas, Galinis Arvydas. District heating in cities as a part of low-carbon energy system[J].*Energy*.2018;152:627-639.
- [10] Zang Haixiang, Geng Minghao, Huang Manyun, Wei Zhingnong, Chen Sheng, Sun Guoqiang. Review and Prospect of State Estimation for Electricity-Heat-Gas Integrated Energy System[J]. *Automation of Electric Power Systems*. 2022; 46(07): 187-199.
- [11] Li Jinghua, Zhu Mengshu, Lu Yuejiang, Huang Yujin, Wu Tong. Review on Optimal Scheduling of Integrated Energy Systems[J]. *Power System Technology*. 2021; 45(06):2256-2272.
- [12] Chen Guoping, Dong Yu, Liang Zhifeng. Analysis and Reflection on High-quality Development of New Energy With Chinese Characteristics in Energy Transition[J]. *Proceedings of the CSEE*. 2020; 40(17):5493-5506.
- [13] Luo Zhao, Liu Dewen, Shen Xin; Wang Gang, Yu Pingqin, Li Zhao. Review of Research on Optimal Operation Technology of Integrated Energy System[J].*Electric Power Construction*. 2022.43(12):3-14.
- [14] Lyu Jiawei, Zhang Shenxi, Cheng Haozhong, Han Feng, Yuan Kai, Song Yi, Fang Sidun. Review on District-level Integrated Energy System Planning Considering Interconnection and Interaction. *Proceedings of the CSEE*. 2022;46(07):187-199.
- [15] Wang Mingjun, Mu Yunfei, Meng Xianjun, Jia Hongjie, WANG Xudong, HUO Xianxu. Optimal Scheduling Method for Integrated Electro-thermal Energy System Considering Heat Transmission Dynamic Characteristics[J]. *Power System Technology*.2020; 44(01): 132-142.
- [16] Zeng Aidong, Wang Jiawei, Zou Yuhang, Wan Yaheng, Hao Sipeng, Yuan Yubo. Multi-time-scale Optimal Scheduling of Integrated Energy System Considering Heat Storage Characteristics of Heating Network[J]. *High Voltage Engineering*. 2023; 49(10): 4192-4202.
- [17] Li Hairun, Mu Yunfei, Jia Hongjie, Yu Xiaodan, Zhang Jiarui, Tang Zhipeng. Optimal Scheduling of Multi-regional Integrated Power and Heating System Considering Quantified Thermal Storage[J]. *Proceedings of the CSEE*. 2021;41(S1):16-27.
- [18] Li Yongqiu, Xu Jin, Wang Keyou. Dynamic Simulation Algorithm of Integrated Energy System Natural Gas Network Based on Time-domain Two-port Model[J/OL]. *Proceedings of the CSEE*. 2023; doi:10.13334/j.0258-8013.pcsee.230419.
- [19] Tian Weikun, Yu Hao, Li Peng, Ji Haoran, Wang Chengshan. Projective integration-based dynamic simulation method for community integrated energy system with gas-electricity coupling[J]. *Electric Power Automation Equipment*. 2020;40(11):40-50.
- [20] Zhai Jiang, Zhou Xiaoxin, Li Yalou, Li Fang, Yang Xiaoyu. Research on Control Strategy of Pressure and Flow of Natural Gas Pipeline in Integrated Energy System[J]. *Proceedings of the CSEE*. 2022,42(11):3911-3924.
- [21] Zhong Junjie, Li Yong, Zeng Zilong, Cao Yijia. Quasi-steady-state analysis and calculation of multi-energy flow for integrated energy system[J]. *Electric Power Automation Equipment*. 2019; 39(08):22-30.
- [22] Liu Xinrui, Li Yao, Sun Qiuye, Pan Yilin. Interaction and Joint State Estimation of Electric-gas-thermal Coupling Network[J]. *Power System Technology*. 2021, 45(02):479-490.
- [23] Wang Yingrui, Zeng Bo, Guo Jing, Shi Jiaqi, Zhang Jianhua. Multi-Energy Flow Calculation Method for Integrated Energy System Containing Electricity, Heat and Gas[J]. *Power System Technology*. 2016; 40(10):2942-2951.